

# Grafting polymers to titania nanoparticles by radical polymerization initiated by diazonium salt

Alice Mesnage · Mohamed Abdel Magied ·  
Pardis Simon · Nathalie Herlin-Boime ·  
Pascale Jégou · Guy Deniau · Serge Palacin

Received: 30 March 2011 / Accepted: 10 June 2011 / Published online: 21 June 2011  
© Springer Science+Business Media, LLC 2011

**Abstract** The grafting of biocompatible poly(hydroxyethyl) methacrylate (PHEMA) by a very simple method onto titanium dioxide nanoparticles is reported. The selected grafting process is based on the chemical reduction of diazonium salts by reducing agents in presence of the vinylic monomer. As previously demonstrated on flat surfaces, it leads to strongly grafted and stable polymer films and has many advantages residing in a short one-step reaction occurring at atmospheric pressure, ambient air and room temperature in water. TiO<sub>2</sub> nanoparticles were synthesized by laser pyrolysis, giving nanoparticles with controlled size and composition. The coating, the composition, the chemical structure, and the grafted PHEMA quantities of the resulting products were investigated by Transmission electron microscopy, Infrared-attenuated total reflection, X-ray photoelectron spectroscopy, and Thermogravimetric analysis. It was demonstrated that the PHEMA shell was successfully chemically grafted onto the surface of the TiO<sub>2</sub> core without any significant influence on the morphology of the nanoparticles.

## Introduction

Titanium dioxide has attracted a great interest due to its unique physico-chemical properties. Highly employed for

various applications such as cosmetics [1], catalysis, pigment industries [2], solar cells [3, 4], and photocatalysis for organic pollutants degradation [5], TiO<sub>2</sub> has also started to be used in the form of films for the immobilization of biomolecules [6] and in the form of nanoparticles in the field of hybrid materials [7–10]. In applications involving TiO<sub>2</sub> nanoparticles, a key parameter is their dispersion with control of aggregation in either various solvents or polymeric matrices. To improve stability and control the dispersion, the organic modification of TiO<sub>2</sub> surface has shown to be efficient since it helps preventing aggregation of the particles and improving their affinity for their environments. In the literature, the main route described for modifying the surface of TiO<sub>2</sub> nanoparticles with organic materials is polymer grafting.

To functionalize the surface of TiO<sub>2</sub> nanoparticles, several approaches have been reported. For instance, the radical graft polymerization of vinyl monomers on the surface of TiO<sub>2</sub> nanoparticles has been successfully achieved by employing radiation [11], high frequency discharge plasma [12] or by introducing trichloroacetyl [13], azo [13, 14], or peroxyester [15] initiating groups in order to initiate the polymerization. The grafting of TiO<sub>2</sub> nanoparticles has also been achieved using usual polymerization initiators with a prior grafting of coupling agents on the nanoparticles such as acrylic acid chloride [14], butyltitanate [16], phosphorus-containing compounds [10, 17], or more commonly double bonds-terminated silyl products [9, 18, 19]. Most of the cited works focused on the grafting of methacrylate polymers (in particular poly(methyl methacrylate) PMMA). Few teams dealt with the grafting of poly(styrene) [10, 12, 14, 17], poly(ethyleneterephthalate) [7, 8], or poly(tetraethylene glycol malonate) [20] according to the applications of the final nanocomposite. However, all those polymerization processes, successfully used for the surface modification of TiO<sub>2</sub> nanoparticles, going from free radical polymerization

A. Mesnage (✉) · M. Abdel Magied · P. Jégou · G. Deniau · S. Palacin  
CEA, IRAMIS, SPCSI Chemistry of Surfaces and Interfaces Group, 91191 Gif-sur-Yvette, France  
e-mail: alice.mesnage@cea.fr

P. Simon · N. Herlin-Boime  
CEA, IRAMIS, SPAM-LFP, CEA-CNRS URA 2453,  
91191 Gif-sur-Yvette, France

[13, 15, 18] (including controlled ones such as SI-ATRP [21], RAFT [14, 22], or NMRP [17]) to in situ polycondensation [7, 8] generally involve: a two-step reaction or long reaction times or heating/cooling steps or controlled atmosphere or organic solvents.

In this context, the objective of this study is to demonstrate the efficiency of the organic modification of  $\text{TiO}_2$  nanoparticles by a simple “green process.” Moreover, the described process does not change the morphology of the nanoparticles, which opens a new route toward the use of this grafted materials for further functionalization by, for instance, biomolecules or for their integration in polymer matrices. Organic polymer films (of poly(hydroxyethyl) methacrylate (PHEMA) in this case) were grafted onto  $\text{TiO}_2$  nanoparticles via a very simple process recently developed in our laboratory [23, 24]. The process (called Graftfast<sup>TM</sup>) is based on the chemical reduction of diazonium salts by reducing agents in presence of a vinylic monomer. The use of such coupling agent in surface modification processes is well-known and these approaches have been recently reviewed by Bélanger and Pinson [25] (with a focus on electrografting methods) and Chehimi et al. [26]. Particularly the grafting of oxide materials [27] as well as various types of nano-objects has been achieved using diazonium salts, for instance carbon nanotubes [28–33], Ti [34] or diamond nanoparticles [35], graphene nanoribbons [36, 37] or silicon [38] and germanium [39] nanowires. Moreover, several authors reported the surface modification by PHEMA grafting prepared using diazonium salt initiators [40–42]. The Graftfast<sup>TM</sup> process, used in this study, leads to stable, homogeneous and covalently grafted polymer films via a short one-step reaction occurring at atmospheric pressure, room temperature, in water and requiring no external energy source. The efficiency of this process has already been demonstrated and its mechanism studied on flat surfaces as well as on carbon nanotubes [23, 24, 43, 44]. In this article, we report the feasibility of such a grafting on  $\text{TiO}_2$  nanoparticles by adapting the experimental conditions. We present here our initial results on the preparation of PHEMA-modified  $\text{TiO}_2$  nanoparticles. The coating, the composition, the chemical structure, and the grafted PHEMA quantities of the resulting products were investigated by Transmission electron microscopy (TEM), Infrared-attenuated total reflection (IR-ATR), X-ray photoelectron spectroscopy (XPS), and Thermogravimetric analysis (TGA).

## Experimental

### Materials

All the experiments were conducted in deionized water (DI water). All standard chemicals were purchased from

Sigma-Aldrich. In this study, the diazonium salt was nitrobenzenediazonium tetrafluoroborate (NBD, 97%), the vinylic monomer was 2-hydroxyethyl methacrylate (HEMA, 97%), the reducing agent L-ascorbic acid or Vitamin C (VC, >99%). Except for NBD, the reactants were used as received; in particular, the vinylic monomer was not distilled to remove commercial inhibitors. Prior to use, NBD was purified by precipitation in diethyl ether. It is important to notice here that we selected NBD, HEMA, and VC to simplify the understanding of the grafting and the conclusions. Indeed, the mechanism of the Graftfast<sup>TM</sup> process has been deeply investigated using those reactants [24]. However, this grafting technique can also be carried out in organic solvents (with an appropriate choice of the reducing agent) with no restriction on the vinylic monomers [23] and the diazonium salt.

We worked with two kinds of  $\text{TiO}_2$  nanoparticles. The commercially available  $\text{TiO}_2$  nanopowder Evonik Degussa P25 (80 % anatase and 20 % rutile) with a mean diameter of 25 nm was used since it is widely employed in the literature and therefore comparisons can be made. Some of the work was also carried out with  $\text{TiO}_2$  nanoparticles  $12 \pm 3$  nm in diameter (size measured by TEM) synthesized by laser pyrolysis [45–47] consisting of 85% anatase and 15% rutile. The laser pyrolysis method is based on the interaction of a powerful IR laser beam with a mixture of liquid precursors (titanium *tetra*-isopropoxide TTIP for  $\text{TiO}_2$  nanoparticle synthesis). It appears as a highly versatile method for the continuous synthesis of extremely pure and small particles with a narrow size distribution. The variable reaction conditions (temperature, pressure, flow rate...) are also an advantage as they allow synthesizing controlled-size nanoparticles with specific composition; the ratio of anatase and rutile phases can be chosen through the synthesis conditions, with a ratio varying from less than 10–100% [46]. In the following, unless otherwise mentioned, the term  $\text{TiO}_2$  nanoparticles will refer to nanoparticles synthesized from laser pyrolysis.

### Characterization and instrumentation

Infrared spectra were obtained on a Bruker VERTEX 70 spectrometer equipped with ATR (Attenuated Total Reflection) Pike-Miracle device. The detector was a MCT working at liquid nitrogen temperature. The spectra were obtained after 256 scans at  $2\text{ cm}^{-1}$  resolution.

X-ray photoemission spectroscopy analyses were performed with a Kratos Axis Ultra DLD using a high-resolution monochromatic Al-K $\alpha$  line X-ray source at 1486.6 eV. Fixed analyzer pass energy of 20 eV was used for core level scans. The photoelectron take-off angle was always normal to the surface. A survey spectrum and core level spectra of C1s (282–295 eV), O1s (526–538 eV), N1s (396–409 eV),

and Ti2p (455–470 eV) regions were systematically recorded. When charging phenomena occurred, the charge was counterbalanced by adjusting the carbon–carbon bond energy of the contamination of untreated  $\text{TiO}_2$  at 285.0 eV. Vision 2 Manager software was used for digital acquisition but data were processed with Avantage software.

Differential thermogravimetric analyses were carried out on a simultaneous TGA–DSC analyzer Netzsch STA 449 C under a flow of argon and with the following temperature program: 20 to 800 °C at 10 °C/min.

TEM images were obtained with a Philips CM12 electron microscope. For the visualization of the polymer on the nanoparticles, a negative staining was performed by exposing the grids to a drop of a 2 wt% uranyl acetate solution in water for 1 min. The grids were tapped dry with a piece of filter paper to remove the excess stain and air-dried before TEM measurements.

#### Functionalization of $\text{TiO}_2$ nanoparticles with polymer

The mechanism of the Graftfast™ process for the grafting of methacrylate polymer onto  $\text{TiO}_2$  nanoparticles is described in Fig. 1. Originally proposed by Mévellec et al. [23] and recently more detailed [24], it relies on the chemical reduction of diazonium salt, in presence of a vinylic monomer, into aryl radicals (Fig. 1i) which are then able, on the first hand, to form a grafted polyphenylene-like film on the substrate (Fig. 1ii) and, on the other hand, to initiate the radical polymerization of the monomers (Fig. 1iii). Then, the growing radical oligomers eventually graft on the aryl rings present on the surface (Fig. 1iv) to form a grafted polymer shell around the  $\text{TiO}_2$  core. Therefore, the

Graftfast™ process does not lead to the grafting of homopolymers but of statistical copolymers containing the monomer and aryl groups [48]. It is worth noting that this behavior might have an effect on the hydrophilic/hydrophobic properties of the polymer grafts, if the relative amount of aryl groups in the copolymer were significant.

Typically, a 10 mg/mL  $\text{TiO}_2$  nanoparticles solution in 5 °C cooled water was sonicated with an ultrasonic probe for 30 min (rated power of 750 W) [49]. To start the reaction, the diazonium salt (concentration in the suspension of 0.05 M), HEMA and the reducing agent were added in this order with the respective ratio of 1, 15, and 0.1. The suspension was kept under sonication (same settings as above) during the whole 15 min of reaction. To stop the reaction, a volume of ethanol corresponding to at least the initial volume of the reactive solution was added. The suspension was then centrifuged (3000 rpm for 20 min), decanted, and rinsed several times first with ethanol to remove free polymer chains and unreacted monomers, then with dimethyl formamide (DMF) to remove the ungrafted polyphenylene moieties and finally with water to eliminate DMF. Afterward, the Graftfast treated  $\text{TiO}_2$  nanoparticles (GF- $\text{TiO}_2$ ) were either dried in air for a few hours in order to perform IR-ATR, XPS, or TGA measurements, or redispersed in water by 30 min US probe sonication to obtain a suspension to be deposited on TEM grids.

#### Results and discussion

The PHEMA-grafted  $\text{TiO}_2$  nanoparticles (GF- $\text{TiO}_2$ ) prepared by this process were first studied by Infrared

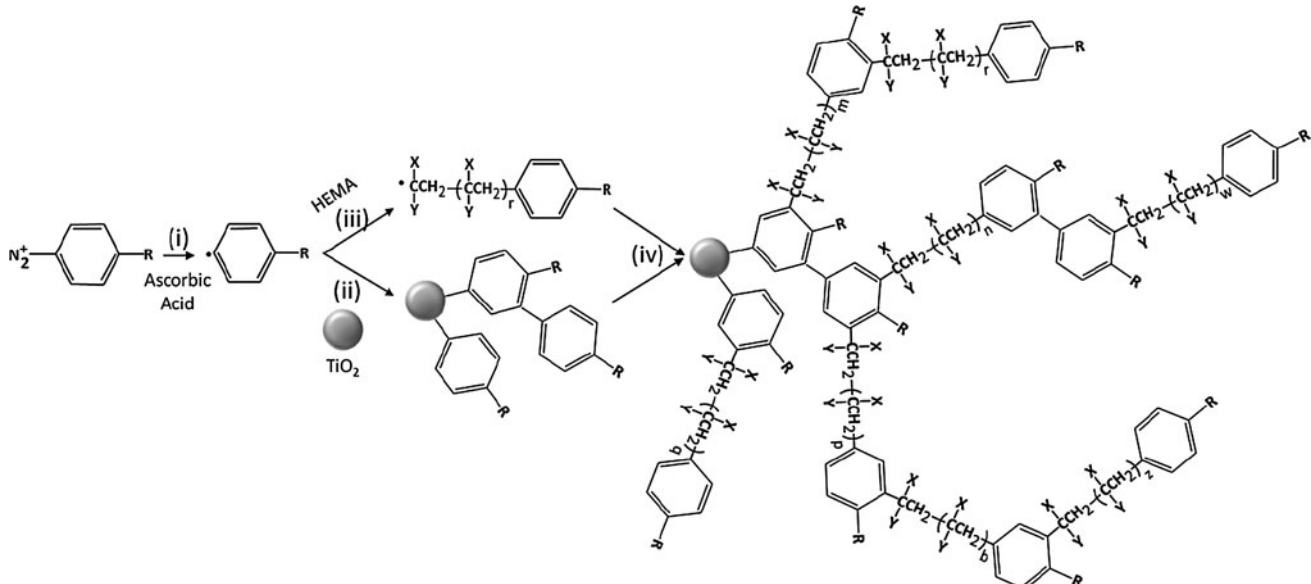


**Fig. 1** Mechanism of a methacrylate polymer grafting onto  $\text{TiO}_2$  nanoparticles by the Graftfast process

spectroscopy. Their IR spectrum is compared to the corresponding untreated  $\text{TiO}_2$  nanoparticles in Fig. 2a and to commercial PHEMA in Fig. 2b. Figure 2a shows that untreated  $\text{TiO}_2$  nanoparticles only absorb at  $3340\text{ cm}^{-1}$  (which corresponds to the stretching motion of the surface hydroxyl groups or the absorption of water), at  $1640\text{ cm}^{-1}$  which can be attributed to the bending vibration of the H–O–H bonds of adsorbed water and show a strong and broad peak in the  $800$ – $600\text{ cm}^{-1}$  region belonging to the lattice vibrations of  $\text{TiO}_2$  nanoparticles. In the grafted GF- $\text{TiO}_2$  product, a new peak at  $1717\text{ cm}^{-1}$  appears. It is due to the stretching vibration of C=O groups contained in the polymer indicating the presence of grafted PHEMA onto  $\text{TiO}_2$  nanoparticles. The comparison of GF- $\text{TiO}_2$  and commercial PHEMA spectra (Fig. 2b) shows very similar absorption bands particularly in the region of  $1270$ – $1120\text{ cm}^{-1}$  (C–O stretching bands) and at  $1720\text{ cm}^{-1}$  (stretching vibration of C=O groups) which confirms the grafting of PHEMA onto  $\text{TiO}_2$  nanoparticles. According to the

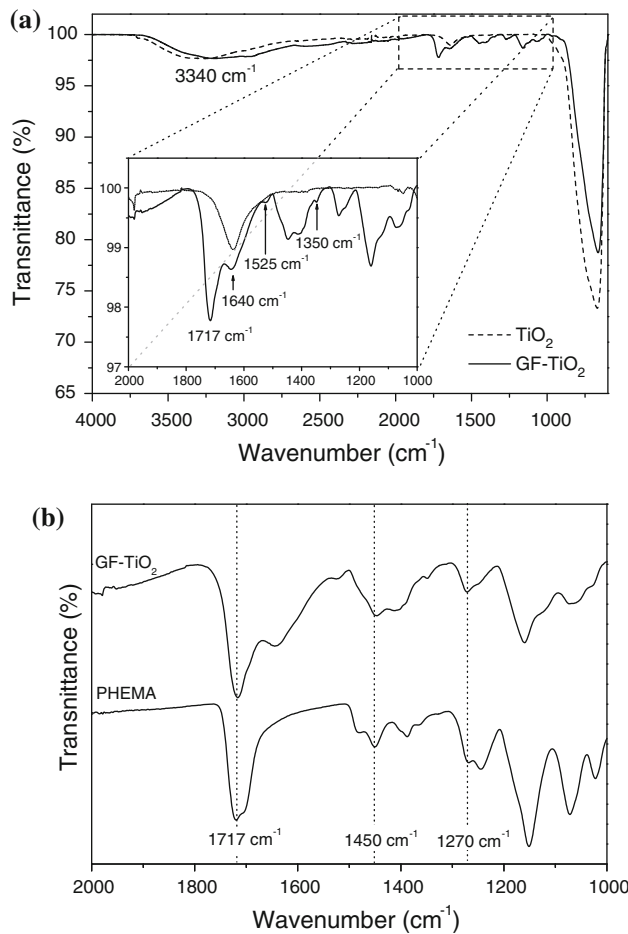


**Fig. 2** IR spectrum of the PHEMA-grafted  $\text{TiO}_2$  nanoparticles (GF- $\text{TiO}_2$ ) compared to **a** the corresponding untreated  $\text{TiO}_2$  nanoparticles (inset in the  $1000$ – $2000\text{ cm}^{-1}$  region) and **b** a commercial PHEMA (20000 g/mol)

mechanism proposed by Mévellec et al. [23] then confirmed by Mesnage et al. [24] (Fig. 1), the GF- $\text{TiO}_2$  spectrum should also exhibit two weak absorption bands at  $1525$  and  $1350\text{ cm}^{-1}$  attributed to, respectively, the asymmetric and symmetric stretching of aryl- $\text{NO}_2$  group which are characteristic of nitrobenzene moieties and a weak peak at  $1600\text{ cm}^{-1}$  typical of the presence of phenyl groups. Those two weak peaks can be clearly seen on the magnification in the  $1000$ – $2000\text{ cm}^{-1}$  region of the IR spectrum presented as inset in Fig. 2a.

XPS analyses were also carried out in order to confirm the efficient grafting of PHEMA onto  $\text{TiO}_2$  nanoparticles. First of all, Fig. 3 shows typical survey scans of untreated and grafted  $\text{TiO}_2$  nanoparticles. Unlike the C1s peak (centered at 285 eV), the main peaks Ti2p and O1s (centered at 459 and 530 eV, respectively) are attenuated in the spectra of the grafted nanoparticles, with respect to the pristine ones. This is the first XPS evidence of the occurrence of a coating. A typical C1s core level spectrum of untreated  $\text{TiO}_2$  nanoparticles (Fig. 4a) is composed of three main peaks. The first contribution was adjusted at 285.0 eV and corresponds to C–C/C–H bonds in alkyl groups ( $-\text{CH}_2$ ,  $-\text{CH}_3$ ). The peak at 286.4 eV is due to  $-\text{C}-\text{O}-$  or  $-\text{C}-\text{N}-$  simple bonds. The last peak at a higher binding energy (288.7 eV) is assigned to carbonyl groups COO. All those contributions in the C1s spectrum are classically observed and attributed to surface contamination of pristine  $\text{TiO}_2$  nanoparticles. Compared to the C1s spectrum of untreated nanoparticles, the broad C1s core level spectrum of GF- $\text{TiO}_2$  nanoparticles (Fig. 4b) is significantly different. The peak-fitting parameters of functional groups in the C1s region are summarized in Table 1. The C–C bonds of alkyl groups,  $-\text{C}-\text{O}-$  or  $-\text{C}-\text{N}-$  simple bonds and carbonyl ester groups O=C=O were observed with an area ratio ( $-\text{C}-\text{O}-$ ,  $-\text{C}-\text{N}-$ , and COO)/(C–C/C–H) 2.3 times higher in

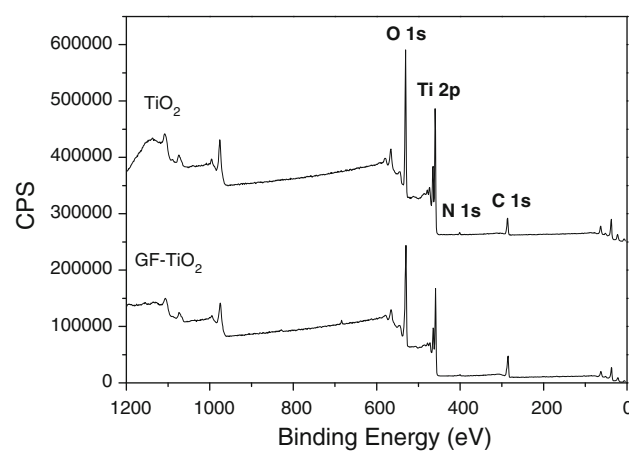


**Fig. 3** Typical XPS survey scans of untreated  $\text{TiO}_2$  nanoparticles ( $\text{TiO}_2$ ) and PHEMA-grafted  $\text{TiO}_2$  nanoparticles (GF- $\text{TiO}_2$ )

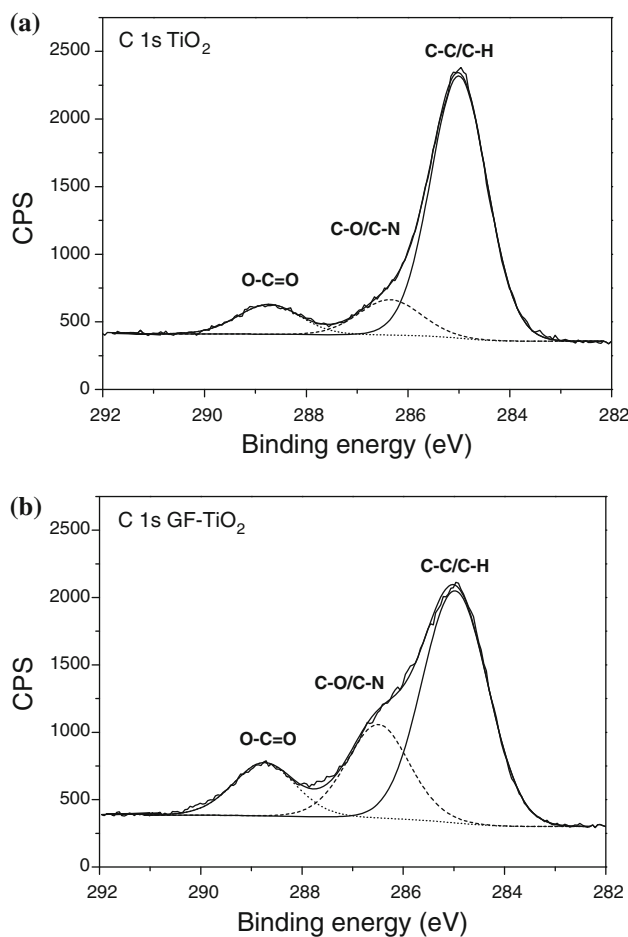


**Fig. 4** Typical XPS C1s core level spectrum of **a** untreated ( $\text{TiO}_2$ ) and **b** PHEMA-grafted  $\text{TiO}_2$  nanoparticles (GF- $\text{TiO}_2$ )

**Table 1** Contributions (in %) of functional groups to C1s regions from untreated ( $\text{TiO}_2$ ) and PHEMA-grafted  $\text{TiO}_2$  nanoparticles (GF- $\text{TiO}_2$ )

	C-C/C-H (285.0 eV)	C-O/C-N (286.4 eV)	O-C=O (288.7 eV)	$\pi-\pi^*$
$\text{TiO}_2$	78.6	11.6	9.8	–
GF- $\text{TiO}_2$	62.1	24.2	13.7	Not visible <sup>a</sup>

<sup>a</sup> It is not surprising that the  $\pi-\pi^*$  shake-up satellite cannot be seen in our experiments since it is likely that in comparison to PHEMA, aromatic rings are present in very low amounts in the polymer film. Therefore, C1s spectra are displayed with a maximum binding energy of 292 eV

GF- $\text{TiO}_2$  spectrum than for the untreated nanoparticles. This is due to the presence of those characteristic groups in the grafted polymer which confirms the grafting of PHEMA on  $\text{TiO}_2$  nanoparticles. The N1s core level in untreated and grafted  $\text{TiO}_2$  nanoparticles was probed (Fig. 5) and revealed that both nanoparticles contain nitrogen. However, the two spectra are clearly different. In the pristine

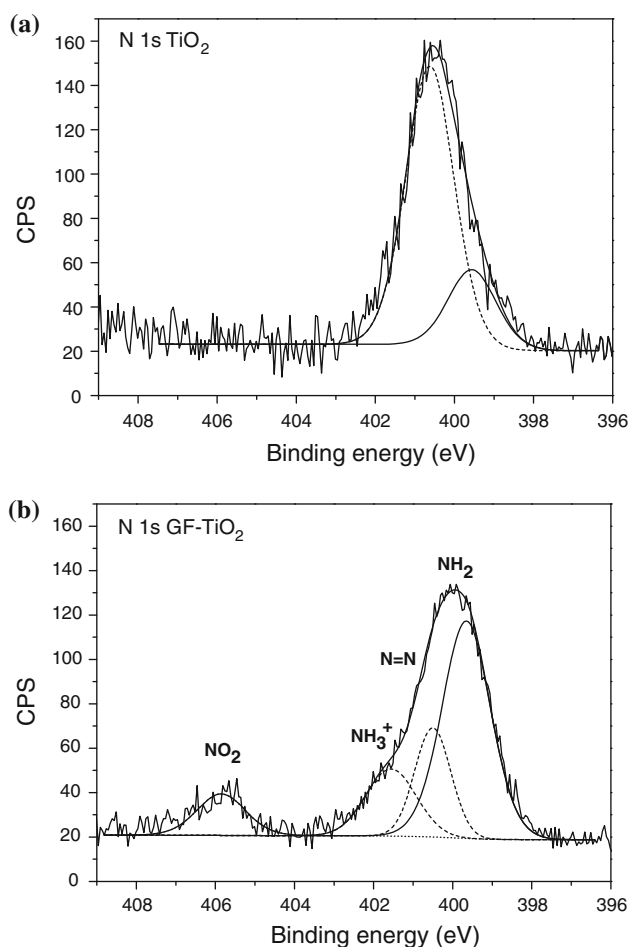


**Fig. 5** Typical XPS N1s core level spectrum of **a** untreated  $\text{TiO}_2$  nanoparticles and **b** PHEMA-grafted  $\text{TiO}_2$  nanoparticles (GF- $\text{TiO}_2$ )

nanoparticles, the two peaks at 399.6 and 400.6 eV are assigned to surface contamination. In the GF- $\text{TiO}_2$ , the first peak at 399.7 eV is assigned to NH<sub>2</sub>, the second peak at 400.5 eV corresponds to nitrogen–nitrogen double bonds (azo groups N=N) while the third peak at 401.6 eV is attributed to NH<sub>3</sub><sup>+</sup> as widely described and discussed in the literature [48, 50–53]. Finally, the peak observed at a higher binding energy (405.9 eV) on the GF- $\text{TiO}_2$  spectrum is assigned to nitro groups (–NO<sub>2</sub>). That latter peak demonstrates clearly the presence of the nitrobenzene moieties in the organic shell grafted onto  $\text{TiO}_2$  nanoparticles and thus confirms the mechanism proposed in Fig. 1. The observed XPS carbon–nitrogen ratio, i.e., (C=O)/(NO<sub>2</sub>)<sup>1</sup> [24], allows us to estimate a grafted PHEMA degree of polymerization (DP) of  $38 \pm 20$  units.

<sup>1</sup> The value of the DP is certainly overestimated. Indeed, nitrogen contamination is present in the pristine nanoparticles. Therefore, it is impossible to take into account the NH<sub>2</sub> groups usually observed in the Graftfast film synthesized with NBD likely to derive from the degradation of the NO<sub>2</sub> groups due to exposure to X-ray irradiation during the XPS analysis [27].

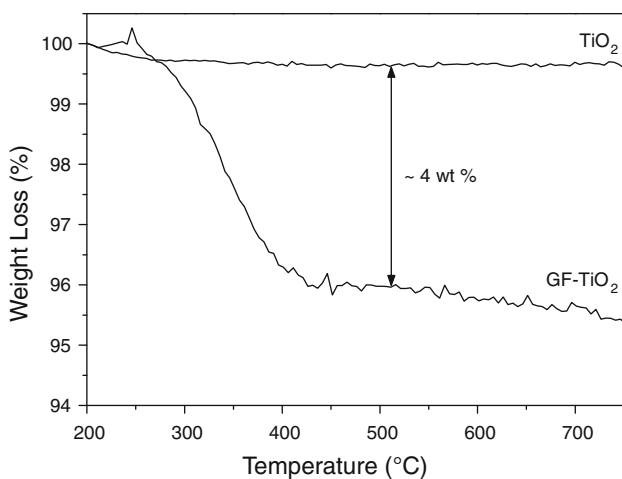


**Fig. 6** TGA curve of pristine and PHEMA-grafted (GF-TiO<sub>2</sub>) TiO<sub>2</sub> nanoparticles

Thermogravimetric analysis was used to estimate the amount of polymer on the TiO<sub>2</sub> nanoparticles surface. Figure 6 shows that the polymer starts to decompose at 250 °C and is completely decomposed at around 500 °C. The data are only given from 200 °C since at lower temperatures the weight of the sample fluctuates. Indeed, these variations, always reported when using this TGA apparatus, come from the introduction of the argon flow in the system which leads to buoyancy on the sample and occur until equilibrium is established. The observed weight loss from 200 to 500 °C indicates that the grafted polymer represents 4.06 wt% of the GF-TiO<sub>2</sub> nanoparticles total weight. From this result, the number of repeating structural units composing PHEMA on the surface of TiO<sub>2</sub> nanoparticles can be estimated. Disregarding nitrophenyl moieties composing the coating, assuming that TiO<sub>2</sub> nanoparticles are individual, that the weight loss can entirely be attributed to the degradation of the polymer and considering that TiO<sub>2</sub> nanoparticles have a density of 3.9 g/cm<sup>3</sup>, we calculate that the TiO<sub>2</sub> nanoparticles are covered by 1.53 ± 0.38 units/nm<sup>2</sup> in average. However, in this calculation, we

did not take into account the aggregation of the nanoparticles which could provide a higher value. Therefore, TGA gives an average coverage ratio of 1–2 HEMA units per nm<sup>2</sup>. This result is in agreement with the low grafting density of polymer chains already indicated by XPS from the attenuation (but not complete extinction) of the Ti2p signal in the survey scans (Fig. 3) of grafted nanoparticles as well as the estimated polymer length of 38 ± 20 units. Besides, combined together, those two estimations indicate that the polymer chains are not grafted at full surface density on the nanoparticle (a grafted polymer chain every 5 nm).

Finally, we tried to observe the grafted polymer around the nanoparticles by TEM. The comparison between the untreated P25 TiO<sub>2</sub> nanoparticles (Fig. 7a) and the corresponding grafted nanoparticles (Fig. 7b) can neither demonstrate the presence of the polymer grafting around the nanoparticles nor lead to a conclusion on the effect of the grafting on their dispersion. Thus, we decided to negatively stain the TEM grid containing the PHEMA-grafted P25 TiO<sub>2</sub> nanoparticles to enhance electron contrast between the polymer and the nanoparticles. The result of the staining is shown in Fig. 7c. The dark gray areas correspond to the polymer which coats the nanoparticles. Therefore, these TEM pictures demonstrate that the polymer has been successfully grafted onto the TiO<sub>2</sub> nanoparticles. It also shows that the morphology of the nanoparticles remains relatively unchanged after grafting.

## Conclusions

This study is the first study on the polymer grafting of TiO<sub>2</sub> nanoparticles by a “green process” based on diazonium salts initiating radical polymerization. The advantages of that method have been demonstrated and lie in a simple setting up and a reaction under non-drastic conditions (short one-step reaction occurring at atmospheric pressure, ambient air, and room temperature). In this preliminary

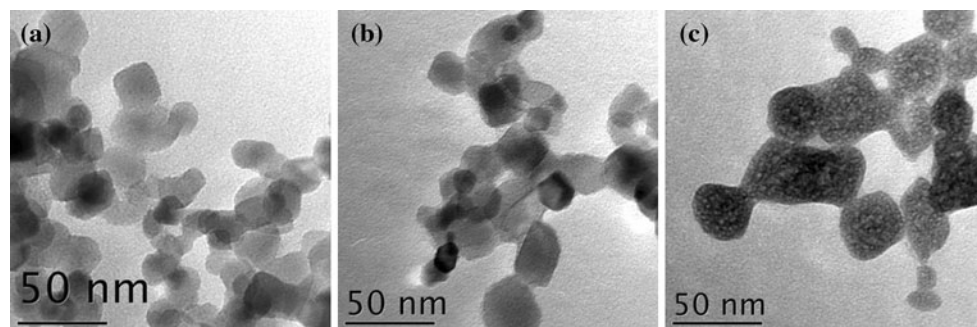


**Fig. 7** TEM images of **a** untreated P25 TiO<sub>2</sub> nanoparticles, **b** PHEMA-grafted P25 TiO<sub>2</sub> nanoparticles, and **c** PHEMA-grafted P25 TiO<sub>2</sub> nanoparticles negatively stained with uranyl acetate

study, we demonstrated the efficiency of the grafting on laser pyrolysis synthesized TiO<sub>2</sub>. TEM images revealed the presence of polymer coated onto the nanoparticles while keeping their morphology. IR-ATR and XPS analyses confirmed the presence but above all the nature of the polymer grafted (PHEMA). XPS also enabled to validate the mechanism involved in the grafting process. Finally, TGA allowed us to estimate the quantity of polymer onto the nanoparticles. Additional study is planned in order to obtain a thicker or more compact grafting of the polymer by adjusting the synthesis parameters. Finally, we strongly believe that this very simple grafting process can be adapted and applied to prepare different types of grafted TiO<sub>2</sub> nanoparticles by changing the diazonium salt and/or the vinylic monomer. Therefore, this surface modification process opens the way for a large number of applications requiring not only polymer-grafted TiO<sub>2</sub> nanoparticles but also other types of polymer-coated nanoparticles.

## References

1. Serpone N, Dondi D, Albini A (2007) Inorg Chim Acta 360:794
2. del Pino AP, Serra P, Morenza JL (2002) Thin Solid Films 415:201
3. Gratzel M (2001) Nature 414:338
4. Oregan B, Gratzel M (1991) Nature 353:737
5. Varghese OK, Paulose M, LaTempa TJ, Grimes CA (2009) Nano Lett 9:731
6. Chen X, Dong SJ (2003) Biosens Bioelectron 18:999
7. El Fray M, Boccaccini AR (2005) Mater Lett 59:2300
8. Han KQ, Yu MH (2006) J Appl Polym Sci 100:1588
9. Zou JP, Zhao Y, Yang MJ, Dan Y (2007) J Appl Polym Sci 104:2792
10. Tchoul MN, Fillery SP, Koerner H, Drummy LF, Oyerokun FT, Mirau PA, Durstock MF, Vaia RA (2010) Chem Mater 22:1749
11. Jiang B, Zu XT, Tang FY, Wu ZH, Lu J, Wei QR, Zhang XD (2006) J Appl Polym Sci 100:3510
12. Zhong SF, Ou QR, Meng YD (2007) J Wuham Univ Technol (Mater Sci Ed) 22:303
13. Shirai Y, Kawatsura K, Tsubokawa N (1999) Prog Org Coat 36:217
14. Lowes BJ, Bohrer AG, Tran T, Shipp DA (2009) Polym Bull 62:281
15. Tsubokawa N, Ishida H (1992) Polym J 24:809
16. Li GH (2009) Surf Rev Lett 16:149
17. Matsuno R, Otsuka H, Takahara A (2006) Soft Matter 2:415
18. Xu H, Shi JX, Sun T (2008) J Adv Mater 40:27
19. Zan L, Liu ZS, Zhong JC, Peng ZG (2004) J Mater Sci 39:3261. doi:[10.1023/B:JMSC.0000025874.78279.f0](https://doi.org/10.1023/B:JMSC.0000025874.78279.f0)
20. Deng C, James PF, Wright PV (1998) J Mater Chem 8:153
21. Fan XW, Lin LJ, Messersmith PB (2006) Compos Sci Technol 66:1198
22. Hojjati B, Charpentier PA (2008) J Polym Sci A 46:3926
23. Mevellec V, Roussel S, Tessier L, Chancolon J, Mayne-L'Hermite M, Deniau G, Viel P, Palacin S (2007) Chem Mater 19:6323
24. Mesnage A, Esnouf S, Jegou P, Deniau G, Palacin S (2010) Chem Mater 22:6229
25. Bélanger D, Pinson J (2011) Chem Soc Rev. doi:[10.1039/c1030cs00149j](https://doi.org/10.1039/c1030cs00149j)
26. Mahouche-Chergui S, Gam-Derouich S, Mangeney C, Chehimi M (2011) Chem Soc Rev. doi:[10.1039/c1030cs00179a](https://doi.org/10.1039/c1030cs00179a)
27. Mendes P, Belloni M, Ashworth M, Hardy C, Nikitin K, Fitzmaurice D, Critchley K, Evans S, Preece J (2003) Chem Phys Chem 4:884
28. Tessier L, Chancolon J, Alet PJ, Trenggono A, Mayne-L'Hermite M, Deniau G, Jegou P, Palacin S (2008) Phys Status Solidi A 205:1412
29. Wu W, Tsarevsky NV, Hudson JL, Tour JM, Matyjaszewski K, Kowalewski T (2007) Small 3:1803
30. Abiman P, Wildgoose GG, Compton RG (2008) Int J Electrochem Sci 3:104
31. Brunetti FG, Herrero MA, Munoz JD, Diaz-Ortiz A, Alfonsi J, Meneghetti M, Prato M, Vazquez E (2008) J Am Chem Soc 130:8094
32. Dyke CA, Stewart MP, Maya F, Tour JM (2004) Synlett 155
33. Schmidt G, Gallon S, Esnouf S, Bourgoin JP, Chenevier P (2009) Chem Eur J 15:2101
34. Ghosh D, Pradhan S, Chen W, Chen SW (2008) Chem Mater 20:1248
35. Dahoumane SA, Nguyen MN, Thorel A, Boudou JP, Chehimi MM, Mangeney C (2009) Langmuir 25:9633
36. Sinitkii A, Dimiev A, Corley DA, Fursina AA, Kosynkin DV, Tour JM (2010) ACS Nano 4:1949
37. Zhu Y, Higginbotham AL, Tour JM (2009) Chem Mater 21:5284
38. Haight R, Sekaric L, Afzali A, Newns D (2009) Nano Lett 9:3165
39. Collins G, Fleming P, O'Dwyers C, Morris MA, Holmes JD (2011) Chem Mater 23:1883
40. Gam-Derouich S, Carbonnier B, Turmine M, Lang P, Jouini M, Ben Hassen-Chehimi D, Chehimi MM (2010) Langmuir 26:11830
41. Matrab T, Nguyen MN, Mahouche S, Lang P, Badre C, Turmine M, Girard G, Bai JB, Chehimi M (2008) J Adhes 84:684
42. Tessier L (2009) PhD thesis (defended in October 2009). University Pierre and Marie Curie, Paris
43. Viel P, Le XT, Huc V, Bar J, Benedetto A, Le Goff A, Filoromo A, Alamarguy D, Noel S, Baraton L, Palacin S (2008) J Mater Chem 18:5913
44. Le XT, Viel P, Jegou P, Garcia A, Berthelot T, Bui TH, Palacin S (2010) J Mater Chem 20:3750
45. Maskrot H, Herlin-Boime N, Leconte Y, Jursikova K, Reynaud C, Vicens J (2006) J Nanopart Res 8:351
46. Pignon B, Maskrot H, Ferreol VG, Leconte Y, Coste S, Gervais M, Pouget T, Reynaud C, Tranchant JF, Herlin-Boime N (2008) Eur J Inorg Chem 6:883
47. Simon P, Pignon B, Miao B, Coste-Leconte S, Leconte Y, Marguet S, Jegou P, Bouchet-Fabre B, Reynaud C, Herlin-Boime N (2010) Chem Mater 22:3704
48. Tessier L, Deniau G, Charleux B, Palacin S (2009) Chem Mater 21:4261
49. Simon-Deckers A, Gouget B, Mayne-L'Hermite M, Herlin-Boime N, Reynaud C, Carriere M (2008) Toxicology 253:137
50. Doppelt P, Hallais G, Pinson J, Podvorica F, Verneyre S (2007) Chem Mater 19:4570
51. Laforgue A, Addou T, Belanger D (2005) Langmuir 21:6855
52. Rosario-Castro BI, Fachini ER, Hernandez J, Perez-Davis ME, Cabrera CR (2006) Langmuir 22:6102
53. Yu SSC, Tan ESQ, Jane RT, Downard AJ (2007) Langmuir 23:11074